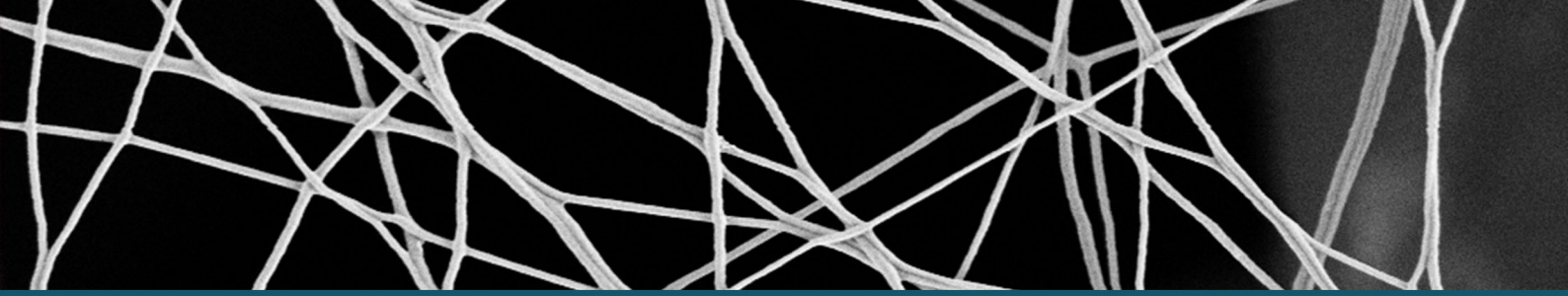

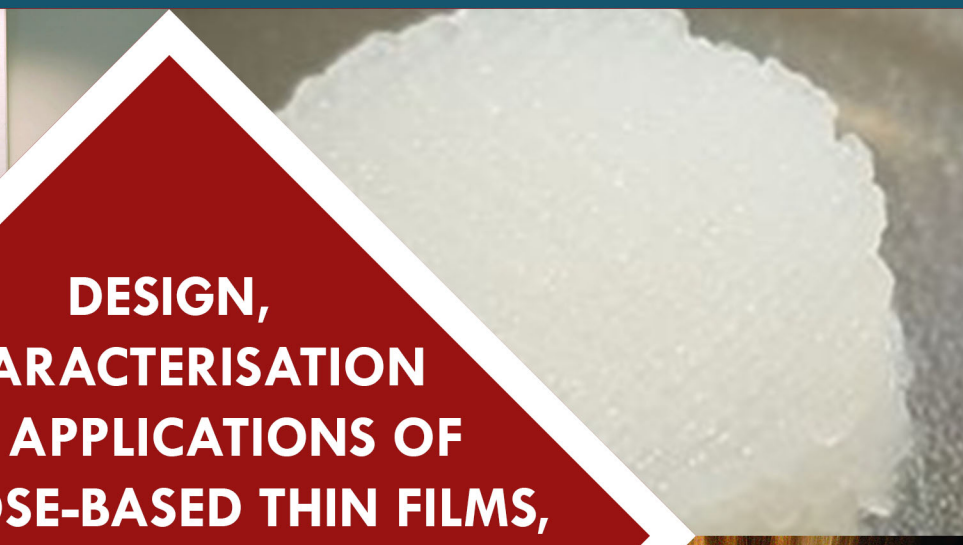

DESIGN, CHARACTERISATION AND APPLICATIONS OF CELLULOSE-BASED THIN FILMS, NANOFIBERS AND 3D PRINTED STRUCTURESV

A Laboratory Manual

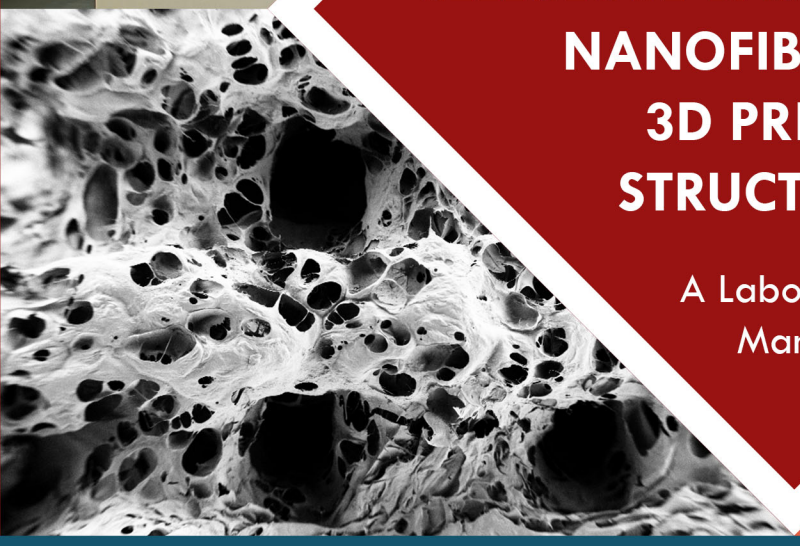

Tanja PIVEC
Tamilselvan MOHAN
Rupert KARGL
Manja KUREČIČ
Karin STANA KLEINSCHEK

University of Maribor Press

University of Maribor

Faculty of Mechanical Engineering

Design, Characterisation and Applications of Cellulose-Based Thin Films, Nanofibers and 3D Printed Structures

A Laboratory Manual

Authors

Tanja Pivec

Tamilselvan Mohan

Rupert Kargl

Manja Kurečič

Karin Stana Kleinschek

February 2021

Title **Design, Characterisation and Applications of Cellulose-Based Thin Films, Nanofibers and 3D Printed Structures**

Subtitle **A Laboratory Manual**

Authors Tanja Pivec
(University of Maribor, Faculty of Mechanical Engineering)

Tamilselvan Mohan
(University of Maribor, Faculty of Mechanical Engineering)

Rupert Kargl
(University of Maribor, Faculty of Mechanical Engineering)

Manja Kurečič
(University of Maribor, Faculty of Electrical Engineering and Computer Science)

Karin Stana Kleinschek
(University of Maribor, Faculty of Electrical Engineering and Computer Science)

Review Lidija Fras Zemljič
(University of Maribor, Faculty of Mechanical Engineering)

Language editing Shelagh Margaret Hedges

Technical editors Tanja Pivec
(University of Maribor, Faculty of Mechanical Engineering)

Jan Perša
(University of Maribor, University Press)

Cover designer Jan Perša
(University of Maribor, University Press)

Cover graphics Manja Kurečič, 3D - © GeSiM mbH & electrospinner © Elmarco.

Graphic material Authors

Published by **University of Maribor**
University Press
Slomškov trg 15, 2000 Maribor, Slovenia
https://press.um.si, zalozba@um.si

Co-published by **University of Maribor**
Faculty of Mechanical Engineering
Smatnova ulica 17, 2000 Maribor, Slovenia
https://www.fs.um.si, fs@um.si

Edition 1st

Published at Maribor, February 2021

Publicagtion type E-book

Available at https://press.um.si/index.php/ump/catalog/book/540

CIP - Kataložni zapis o publikaciji
Univerzitetna knjižnica Maribor

677.017(076)(0.034.1)

DESIGN, characterisation and applications of cellulose-based thin films, nanofibers and 3D printed structures [Elektronski vir] : a laboratory manual / authors Tanja Pivec ... [et al.]. - 1st ed. - E-knjiga. - Maribor : University of Maribor, University Press, 2021

Način dostopa (URL):
https://press.um.si/index.php/ump/catalog/book/540
ISBN 978-961-286-432-3
doi: 10.18690/978-961-286-432-3
COBISS.SI-ID 52101891

ISBN 978-961-286-432-3 (pdf)

DOI https://doi.org/10.18690/978-961-286-432-3

Price Free copy

For publisher prof. dr. Zdravko Kačič,
rector of University of Maribor

Attribution Pivec, T., Mohan, T., Kargl, R., Kurečič, M. in Stana Kleinschek, K. (2021). D*esign, Characterisation and Applications of Cellulose-Based Thin Films, Nanofibers and 3D Printed Structures: a Laboratory Manual.* Maribor: University Press. doi: https://doi.org/10.18690/978-961-286-432-3

University of Maribor Press

Table of Contetns

1 Introduction

1.1 Aim

The aim of this course is to prepare cellulose-based multifunctional materials, which differ in their properties, such as: i) Hydrophobicity/hydrophilicity, ii) Flame retardance, iii) Load-bearing behaviour and iv) Response to changes in the pH value. To do this, cellulose and its derivatives, such as **trimethylsilyl cellulose (TMSC)**, **nanofibrillated cellulose (NFC)**, **carboxymethyl cellulose (CMC)** and **cellulose acetate (CA)** are used as basic materials. To obtain different functionalities of the final materials, different reagents will be dispersed or dissolved in solutions containing cellulose derivatives. The following reagents will be used for these purposes: i) **Citric acid** and **sodium hypophosphite** as flame retardants, ii) **Alkyl ketene dimer (AKD)** as a hydrophobising agent and iii) **Bromocrezol green (halochromic dye)** as a pH indicator. Subsequently, these mixtures will be used in different polymer processing techniques, namely **spin coating**, **electrospinning** and **3D printing.** The obtained structures will be characterised by Contact Angle measurements, rheology, microscopy, spectroscopy and flammability tests, to confirm their functionalities.

1.2 Cellulose and its derivatives for polymer processing

Polymer based materials are omnipresent, and have been used in many areas owing to their attractive properties. These properties include - depending on the type of polymer (e.g. polyethylene (PE), polystyrene (PS), polycarbonate (PC), polylactide (PLA), polyethylene terephthalate (PET)…) durability, good mechanical strength [1, 2], (bio-)compatibility [3], corrosion resistance [4], flame retardance [5] and renewability [6]. As a ubiquitous polymer on earth, **cellulose** is of interest for material processing, and has found useful applications in clothing and construction [7]. However, processing of cellulose can be highly polluting and energy consuming. To exploit cellulose as a source of continued innovation or commercialisation, the latest research and industrial development focus on cleaner, cheaper and superior cellulose processing routes [8]. Cellulose is renewable, nontoxic, and compatible with many organic and inorganic materials [9]. This facilitates the creation of hybrid materials and nanocomposites with unique and very diverse properties and applications, such as conductive fibres, papers with printed circuits, flame retardant or wound dressing materials [9]. Cellulose is the major component in the cell walls of plants and algae, and is secreted by certain bacteria. It can also be found in marine animals called tunicates. Cellulose is a linear syndiotactic homopolymer, consisting of D-anhydroglucopyranose units (AGU), which are connected covalently through β-(1→4)-glycosidic bonds between the carbon atoms C(1) and C'(4) of adjacent glucose units, resulting in a cellobiose unit (see Figure 1.1), which is the main building block of the cellulose polymer.

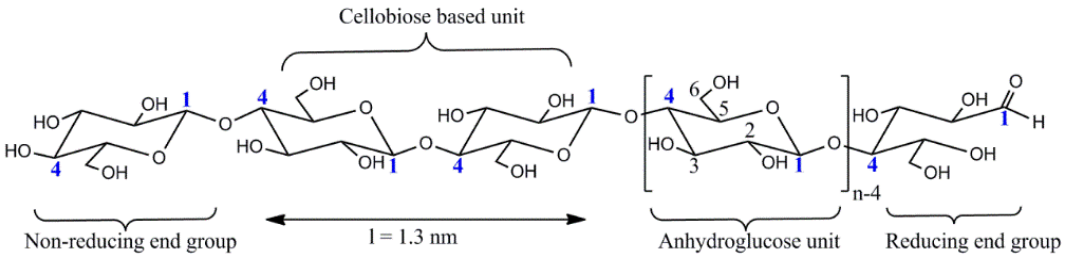

Figure 1.1: Molecular structure of cellulose.

However, the insolubility of cellulose in common organic solvents limits its processibility. This limitation can be overcome by preparing cellulose-based derivatives, which show a good solubility in water or common organic solvents, or which are thermoplastic e.g. flow upon heating and shearing. Cellulose derivatives can be classified broadly into ether and ester derivatives. Here, two different aliphatic ethers, i.e. trimethylsilyl cellulose (TMSC) and carboxymethyl cellulose (CMC) and one ester, i.e. cellulose acetate (CA), will be used

for processing, i.e. spin coating, electrospinning and 3D printing. Nanofibrillated cellulose (NFC) will also be used to provide the strength of the processed cellulose based material (3D printed materials) . NFC is an attractive material building block for the preparation of different composite materials i.e. nanopaper, light-weight aerogels and foams, where it is used for reinforcement of the polymer matrices [10].

Trimethylsilyl cellulose (TMSC)

TMSC is a hydrophobic cellulose derivative, which can be produced by the silylation of hydroxyl groups of the cellulose with hydrophobic trimethylsilyl groups under homogeneous or heterogeneous conditions (Figure 1.2). Depending on the DS (Degree of Substitution, the molar ratio of substituent vs. 3 mol of available hydroxyl groups for substitution at one glucose unit), TMSC is soluble in organic solvents like tetrahydrofuran (THF), hexane, toluene (high DS), or in polar solvents like alcohols and DMSO (low DS). TMSC has been studied extensively due to its potential to regenerate cellulose simply by treatment with acids, that leads to a desilylation of the hydroxyl groups to produce cellulose fibres, particles or films [11-14].

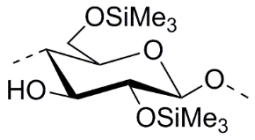

Figure 1.2: Molecular structure of trimethylsilyl cellulose (TMSC).

Carboxymethyl cellulose (CMC)

CMC is a cellulose derivative with carboxymethyl groups (-CH_2-COOH) bound to the hydroxyl groups of the glucopyranose monomers that make up the cellulose backbone (Figure 1.3). It is often used as its water soluble sodium salt (sodium carboxymethyl cellulose).

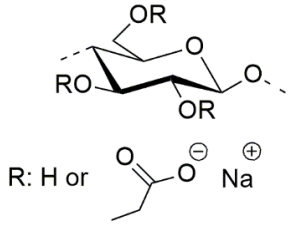

Figure 1.3: Molecular structure of sodium carboxymethyl cellulose.

CMC is an inexpensive, biodegradable and water-soluble polymer, used as a viscosity modifier or thickener [15]. CMC is used for binding of biomacromolecules like proteins cells, and forms hydrogels with alginic acid (ALG) [16]. While the use of CMC, together with polyethylene oxide (PEO), is known to form fibres in electrospinning [17, 18], its application with nano-structured cellulose like nanofibrillated cellulose (NFC) for 3D bioprinting and for creating flame retardant nano-biocomposites are less investigated ,and, thus, still challenging [19].

Cellulose acetate (CA)

A cellulose derivate, often used in electrospinning and for films and membranes` production, is cellulose acetate (CA). It is one of the most important esters of cellulose (Figure 1.4) [20].

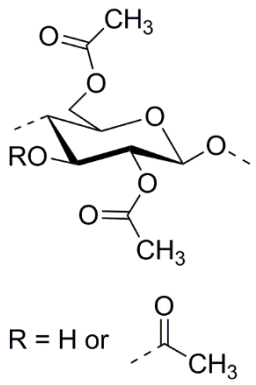

Figure 1.4: Molecular structure of cellulose acetate (DS 2).

Besides its bio-inertness and diverse physicochemical properties, CA is a suitable material for biological applications, as it exhibits low-cytotoxicity. It can form nanofibres in combination with various nanoparticles (metal, ceramic) and active substances by electrospinning from organic solvents [21].

NanofibrilLated cellulose (NFC)

The development of nanocomposites derived from renewable sources with nanocellulose as reinforcement is an intensively investigated area of research. The term 'nanocellulose' generally refers to cellulosic materials having at least one dimension in the nanometre scale. Nanocellulose can be produced by different methods from various lignocellulosic sources [22]. Recently, considerable interest has been directed to cellulose nanofibres

because of their low thermal expansion, high aspect ratio between length and diameter, strengthening effect, and good mechanical and optical properties. These materials may find application in nanocomposites, paper, coatings, additives, security features, food packaging, and as gas barriers [23].

Nanocelluloses can be classified in three main subcategories, based on their dimensions, functions, and preparation methods, which depends mainly on the cellulose source and the processing conditions. Herein, the nomenclature used is cellulose nanocrystal (CNC), nanofibrillated cellulose (NFC) and bacterial nanocellulose (BNC). Although all types are similar in chemical composition, they are different in morphology, particle size, crystallinity, and some properties, due to the difference of sources and extraction methods [24].

NFC consists of bundles of stretched cellulose chain molecules with long, flexible and entangled cellulose nanofibres with an average diameter from 5 to 60 nm and a length of several micrometres (Figure 1.5). They consist of alternating crystalline and amorphous domains. NFC is generally produced by delamination of wood pulp through mechanical pressure before and/or after chemical (i.e. acid hydrolysys, alkaline hydrolysis, treatment with an oxidation agent, organosolv treatment, ionic liquids` treatment) or enzymatic treatment [22, 23].

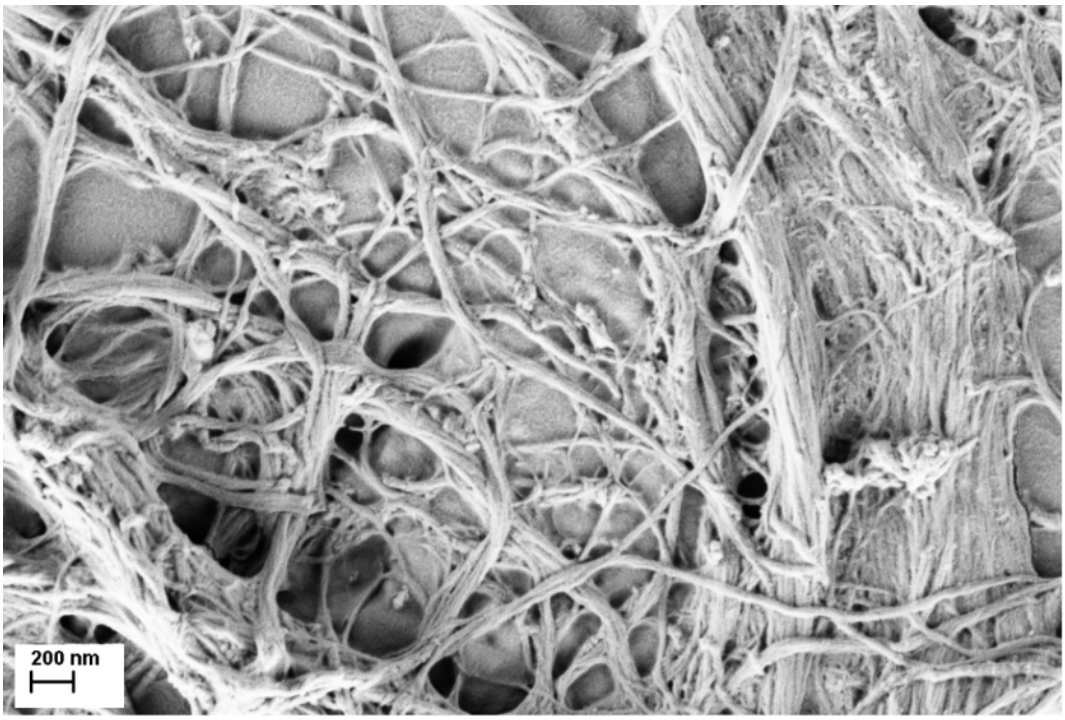

Figure 1.5: SEM micrograph of nanofibrillated cellulose.

CNC is nanocellulose with high strength, which is usually extracted from cellulose fibrils by acid hydrolysis. It has a short-rod-like shape or whisker shape, 2–20 nm in diameter and 100–500 nm in length. Also, it contains 100% of cellulose chemical composition, mainly in crystalline regions (high crystallinity around 54–88% [24].

BNC is another kind of nanocellulose which is different from CNC and NFC. CNC and NFC can be extracted from lignocellulosic biomass (top-down process), but BNC is produced from building up of the low molecular weight of sugars by bacteria, mainly by *Gluconacetobacter xylinus* for a few days up to two weeks (bottom-up process). As such, the BNC is always in the pure form, without other components from lignocellulosic biomass such as lignin, hemicellulose, pectin, and so on. BNC has the same chemical compositions as other two kinds of nanocelluloses. It is in the form of twisting ribbons with average diameters of 20–100 nm and micrometre lengths with a large surface area per unit [24].

1.3 Advanced techniques for processing of cellulose-based materials

Numerous methods have been utilised for polymer processing to obtain materials suitable for a wide variety of applications. Here, three different techniques are presented, and all of them enable the incorporation of different substances into the basic polymer matrix. Spin coating, electrospinning and 3D printing, are presented separately in individual Lab Exercises.

2 Lab exercise 1: Spin coating of cellulose thin films

2.1 Objective

The aim of Lab Exercise 1 is to prepare cellulose thin films using spin coating of TMSC and the regeneration into cellulose using HCl vapours. The success of regeneration will be analysed using Static Water Contact Angle (SWCA) measurements by goniometry.

2.2 Introduction

Cellulose thin films are of interest in fundamental studies and applicative developments, especially in the field of Surface Science. There are several ways of preparing thin cellulose films on a smooth solid substrate. A commonly used method is spin coating. For the preparation of regenerated cellulose films, TMSC can be used as a starting material. After spin coating of TMSC on a flat substrate, the trimethylsilyl groups (TMS) can be removed by exposure to an acidic atmosphere of hydrochloric acid, yielding amorphous cellulose. This procedure is termed regeneration (Figure 2.1)[11].

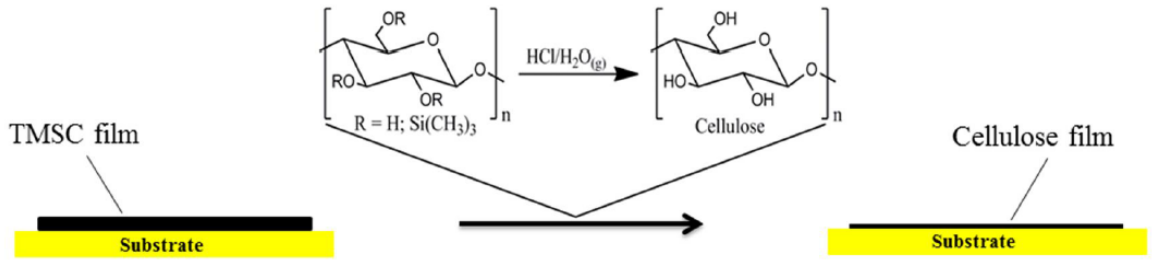

Figure 2.1: Regeneration of cellulose from spin coated TMSC using vapour phase acid treatment [11].

Spin coating is a simple procedure used to apply uniform thin coatings with a thickness ranging from a few nanometres to a few microns to relatively flat substrates. A typical process involves the depositing of a drop of a fluid resin (a solution of the desired material in a solvent) onto the centre of a substrate, and then spinning the substrate at high speed (typically around 500-3,000 rpm). Centrifugal force will cause the resin to spread to, and eventually off, the edge of the substrate, leaving a thin film of resin on the surface. Final film thickness and other properties, such as roughness, will depend on the nature of the resin (viscosity, drying rate, percent solids, surface tension, etc.) and the parameters chosen for the spinning process. Factors such as final rotational speed, acceleration and fume exhaust contribute to how the properties of coated films are defined. Spin coating is used as a model system to study various surface properties (e.g. nano-scaled morphology, wettability) in a nanometre scale, which could otherwise not be done with bulk materials.

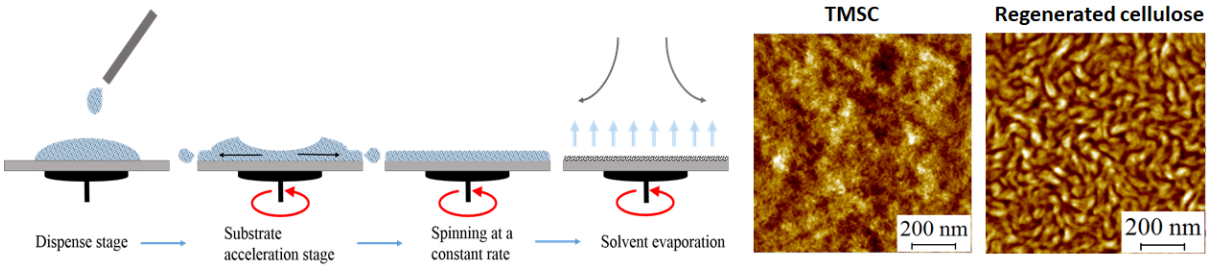

Figure 2.2: Four stages of the spin coating process (left) and spin coated trimethylsilyl cellulose (TMSC) and regenerated cellulose films (right).

The Wettability of the thin films can be measured by Contact Angle measurements using a goniometer. An equilibrium of vectorial forces dictates the Contact Angle Θ_C at the three phase contact line of a deposited drop. The surface energy of the solid σ_S acts along the solid surface. The solid-liquid interfacial energy σ_{SL} acts in the opposite direction, and the surface tension σ_L of the liquid acts tangentially to the drop surface. This can be described by a simple scalar equation, the Young equation:

$$\sigma_L \cos\Theta_C = \sigma_S - \sigma_{SL}$$

The drop is viewed in profile during the Contact Angle measurement by goniometer. The image processing software recognises and records the drop contour, as well as the base line at the solid-liquid interface, and fits a mathematical function to the drop shape [25].

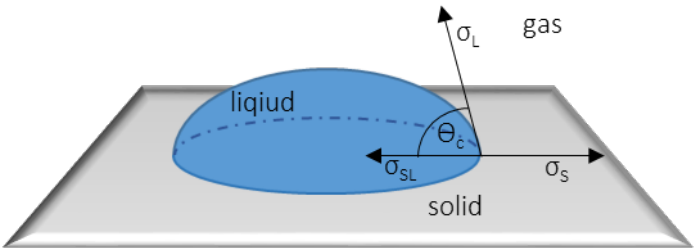

Figure 2.3: Contact Angle at a solid-liquid-gas contact line [25].

The hydrophilicity/hydrophobicity of surfaces can be defined, depending on the measured Water Contact Angle value. Surfaces with a Contact Angle < 90° are referred to as hydrophilic, and those with an angle >90° as hydrophobic. It is worth noting that the described method measures the so-called Static Contact Angle, in contrast to measurements with receding or advancing Contact Angles, where the contact line is changed during the measurements. The difference between the advancing and receding Contact Angles is termed the Contact Angle hysteresis.

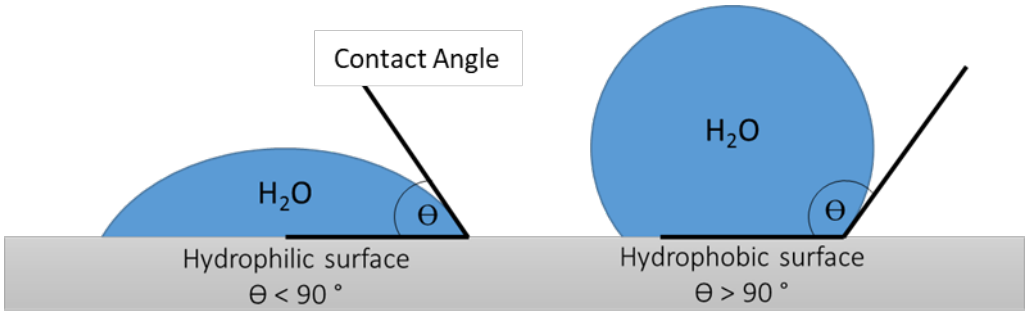

Figure 2.4: Hydrophilic and hydrophobic surfaces.

2.3 Experimental section

Materials required

The chemicals and materials needed for cellulose thin film preparation and characterisation are listed below:

- Trimethylsilyl cellulose (TMSC) with a DS_{TMS} of 2.55, (M_W = 175,000 g/mol, M_n = 36,000 g/mol) synthesised from microcrystalline cellulose (Avicel) (Friedrich Schiller University Jena)
- Toluene (99.9 %) (Sigma-Aldrich)
- Hydrochloric acid (HCl, 37 %) (Sigma-Aldrich)
- Silicon wafers (Topsil, Germany)
- Polystyrene Petri Dishes (4 cm in diameter)
- Milli-Q water from a Millipore water purification system (Millipore, USA; resistivity = 18.2 MΩ·cm)

Preparation of spin coated films

Solution preparation: Dissolve the TMSC in toluene at a concentration of 10 g/L. For the cellulose regeneration prepare 10 wt. % HCl solution with dilution from 37 % HCl.

Substrate preparation: Prior to spin coating, cut the silicon wafers into pieces of 1.5 x 1.5 cm^2.

Spin coating: Use the spin coater (MCD-200-NPP spin coater from Polos, Germany) for preparation of thin films on the surfaces of silicon wafers. Deposit 50 µl of TMSC solution on the static substrate (silicon wafer), then rotate it for 60 s at a spinning rate of 4000 rpm and an acceleration of 2500 rpm.

Regeneration: Regenerate the spin coated TMSC to cellulose by vapour phase acid hydrolysis. Briefly, place each TMSC coated substrate separately in a 20 mL polystyrene Petri Dish (4 cm in diameter). Then, place a volume of 3 mL of 10 wt. % HCl beside the coated substrate (the liquid must not touch the silicon wafer) and cover the Petri Dish with its cap. Regenerate the surface of thin films for 10 minutes at room temperature. After the regeneration, pipette the acid from the Petri Dishes carefully and store the silicon

wafers with regenerated TMSC thin films in fresh Petri Dishes, at room temperature. Do not touch the silicon wafers with the fingers - use tweezers for gripping and movingthem.

Analytical methods

Static Water Contact Angle (SWCA) measurements

Define the hydrophilic/hydrophobic properties and the success of regeneration, based on the SWCA measurements for the TMSC thin films and regenerated cellulose thin films. Briefly, define the wettability of the spin coated samples by measuring the Water Contact Angle (Milli-Q water, drop volume 3 μl) formed between a liquid drop and a solid surface, using a goniometer OCA15+ (Dataphysics, Germany). The SWCA will be determined based on the analysis of the drop shape (Young-Laplace approach) using the software provided by the manufacturer (software version SCA 20.2.0). All the measurements should be performed on each sample with a minimum of five drops per surface, and the average and Standard Deviation should be calculated.

2.4 Results and discussion

Make a comparison between the measured SWCA values for TMSC and cellulose films. Give the measured values in the form of a Table or graph. Define the hydrophobic/hydrophilic properties of both films. How is the hydrophobic/hydrophilic character changed after regeneration of TMSC film? Why is the hydrophobicity /hydrophilicity of a thin film surface changed after regeneration with acid hydrolysis?

3 Lab exercise 2: Electrospun nanofibrous mats

3.1 Objective

The aim of Lab Exercise 2 is to prepare pH-indicating cellulose-based nanofibrous mats using electrospinning of CA with an included pH-value indicator (BromoCresol Green BCG). The material's colour change after dipping it into solutions with different pH-values will be observed by naked eye, and evaluated in terms of the CIE L*a*b* colour system. The purpose of the prepared material is related to the detection of acidic or alkaline pH-values of wounds and diagnostic purposes.

3.2 Introduction

Electrospun nanofibrous mats have found application in many areas. Among others, electrospinning is of interest for the preparation of wound dressings and for Tissue Engineering [26]. In wound healing, the use of electrospun nanofibrous materials can have a positive effect on the proliferation of cells. Its 3D structure, morphology and physicochemical properties can mimic the characteristics of the Extracellular Matrix (ECM) of the skin cells. Additionally, the incorporation of different substances into the polymer solution and, consequently, in nanofibres, enables preparation of advanced wound dressings with different properties, such as the controlled release of substances that promote wound healing. With the incorporation of pH indicator dyes (halochromic

chemical compounds) it is possible to prepare materials that respond to changes in the pH value of wounds. Such changes occur due to bacterial infections, or the different phases of healing. Open wounds characteristically have a neutral to alkaline pH, existing in the pH range of 6.5 to 8.5, while chronic wounds exist at a range of 7.2 to 8.9. Monitoring pH can help predict the progression of wound healing, as the pH of a wound can be indicative of the biochemical processes of healing. Initially, the wound undergoes acidosis, with increased lactic acid and oxygen in the wound decreasing the pH. Acidosis of the wound is required for the proliferation of fibroblasts, DNA cell synthesis, oxygenation, collagen formation, angiogenesis and macrophage activity. Acidic wound fluid has been associated with more rapid wound healing; however, chronic wounds exist in an alkaline environment. An alkaline wound environment impairs the healing and immunological response by promoting bacterial growth, increasing proteolytic activity, inhibiting fibroblasts and decreasing the oxygen supply [27]. The integration of sensors into electrospun nanofibres is also of interest in the areas of Smart Packaging [28], Textiles [29], Tissue Engineering and microbiological studies [30].

Electrospinning is a technique that uses strong **electrostatic forces** to produce fine fibres from polymer solutions or melts. Fibres produced with electrospinning have a **small diameter** (from nano- to micrometre) and an **exceptionally higher surface area** per mass unit than those obtained with conventional spinning processes. The typical set-up of an electrospinning apparatus consists of three major components: A **feeding unit** (e.g. pipette dip), **high voltage power supply** (15–25 kV) and **a grounded collecting plate** (usually a metal screen or plate that can be covered with a fabric, or a rotating spindle). Nanofibres can be electrospun from synthetic or natural polymers and their blends, optionally containing various additives (metal and ceramic nanoparticles, active substances etc.) to provide additional fibre functionality. Electrospinning has become an important part of research involving technical textiles, shielding materials, air and oil filters, agro- and many medical textiles [31]. Electrospun fibres with flame retardant properties have potential application in the production of rechargeable batteries, photovoltaic cells, and flame retardant textiles [32]. Conventional electrospinning often uses a single or multi needle **set-up** to produce nanofibres. However, this method suffers from a low productivity, typically less than 0.3 g/hr. The main reason is that each needle generates only one polymer jet. In contrast to that, **needleless electrospinning** appeared as an alternative technology, with the aim of producing nanofibres on a larger scale. Needleless electrospinning produces nanofibres directly from an open liquid surface. Numerous jets are formed simultaneously from the fibre generator, without the influence of strong

capillary effects that are normally associated with a needle spinner [33]. An example of CMC/PEO electrospun fibres is given in Figure 3.1.

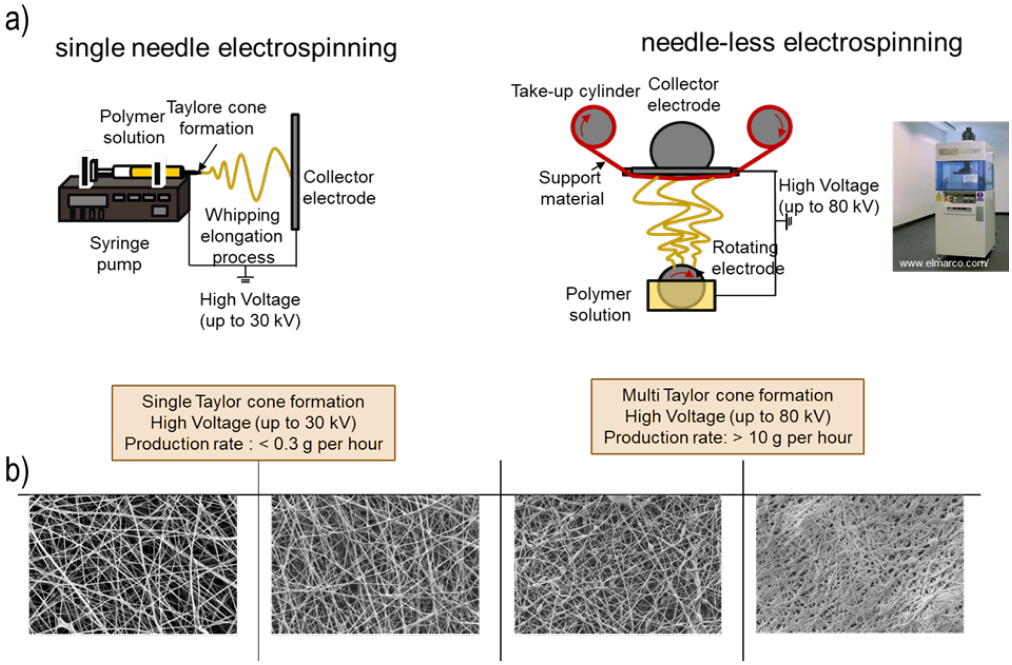

Figure 3.1: Set-up of electrospinning apparatus for single needle and needle-less electrospinning (a); SEM micrographs of CMC/PEO nanofibre mats electrospun with different crosslinker (polycarboxylic acid) concentration with needle-less eletrospinning (b).

To prepare pH-indicating nanofibrous mat, **Bromocrezol Green (BCG) a pH indicator,** will be included in a CA solution and electrospun. The chemical structure of BCG is presented in Figure 3.2. Bromocresol Green is a widely used and well-known pH indicator dye, showing a clear and unambiguous colour change with an observed change in pH. In aqueous solution, Bromocresol Green ionises to give the monoanionic form (yellow), that further deprotonates at higher pH to give the dianionic form (blue), which is stabilised by resonance:

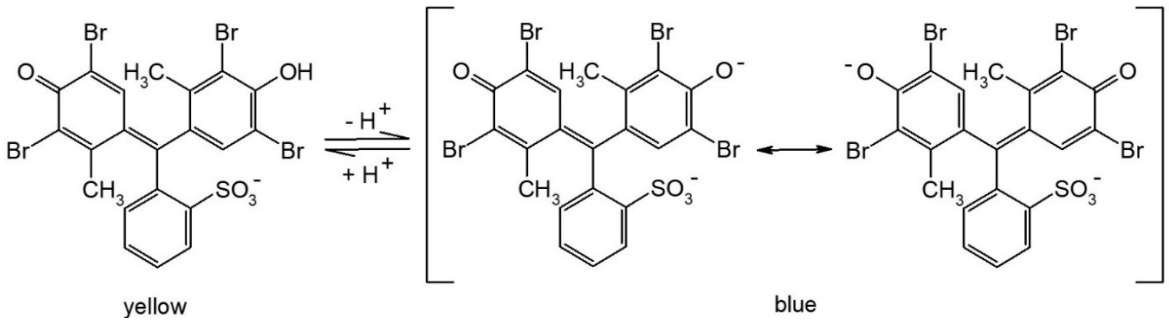

Figure 3.2: Chemical structure of Bromocrezol Green.

The colour of samples could be evaluated in terms of the **CIE L*a*b* colour system,** where L*, a* and b* are the coordinates of the colour in the mathematical combination of a Cartesian and cylindrical coordinate system, based on the theory that colour is perceived as L* (lightness, from 0 for absolute black up to 100 for a perfect white), a* (green—negative axis and red—positive axis), and b* (blue— negative axis and yellow—positive axis) (Figure 3.3) [34].

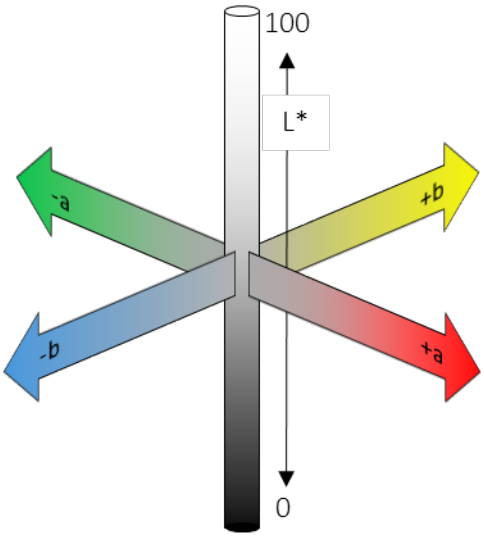

Figure 3.3: CIELab system.

3.3 Experimental section

Materials required

The chemicals and materials needed for preparation and characterisation of pH-indicating nanofibrous mats are listed below:

- Cellulose acetate (CA, M_n=30.000 by GCP, acetyl content: 39.8 wt%)
- Acetic acid (AcOH, ≥ 99.8%), (Sigma-Aldrich)
- Bromocrezol Green (BCG, commercial grade), (Kemika)
- Buffer solutions with pH 2, 4, 7, 9 and 10 (Fluka)
- Milli-Q water from a Millipore water purification system (Millipore, USA; resistivity = 18.2 MΩ·cm)
- Mechanical stirrer

- Pegatex® S non-woven (100% polypropylene fibres), PEGAS NONWOVENS s.r.o. (Znojmo, Czech Republic) needed as mat for nanofibre deposition.

Preparation of electrospun nanofibrous mats

Solutions` preparation: Prepare 200 g of 17 wt.% CA solution. Briefly, dissolve 17 wt.% CA in 85 % AcOH under stirring with a mechanical stirrer (2,000 rpm) until a homogenous solution is obtained (reference). Then, add 0.5 wt.% of BCG, relative to the CA mass to 100 g of CA solution (0,085 g of BCG in 100 g CA solution), and stir it for approx. 2h.

Electrospinning: For the production of nanofibrous mats from the reference CA solution and the CA solution with BCG, use a pilot scale apparatus Nanospider™ NS500 (Elmarco, Czech Republic). For the electrospinning process, use the small wire electrode, and fill the electrode box (sample bath) with approx. 30 mL of CA solution. Then vary the process parameters, such as voltage (from 60 to 75kV) and electrode distance (from 150 to 190 mm), and define the optimal spinning procedure conditions. The time of electrospinning should be at least 30 min.

Analytical methods

Characterisation of polymer solutions: Before electrospinning, measure the solution properties of the CA solution and dye containing CA solution. The viscosity, conductivity and surface tension of the polymer solution are important for the electrospinning process, and for the subsequent morphology of the nanofibres. Measure the viscosity with a rotational viscometer from Fungilab (model Smart series, Barcelona, Spain). Measure the conductivity using a conductivity meter Seven Multi from Mettler Toledo International, Inc., Greifensee, Switzerland. Measure surface tension with a Tensiometer Krüss K-12, Germany according to the Wilhelmy plate method.

Characterisation of electrospun mats: Analyse (with the naked eye) the halochromic behaviour of the electrospun nanofibrous mat incorporated with BCG by dipping the sample for approximately 10 s into individual buffer solutions with a pH varied from 2 to 10. Also, evaluate the colour change with CIE Lab colour measurements in a spectral range of 400-700 nm wavelengths, by means of a two-ray Spectraflash SF600 Plus

spectrophotometer (Datacolor) under a standard illuminant D56 (LAV/Spec.Incl.), and a measuring geometry of s/8°.

Check the reproducibility of the colour change after cyclic immersing of one piece of electrospun nanofibres` sample in the buffers with different pH values, by dipping the electrospun nanofibres in a buffer solution with pH 9, then in pH 4, and repeat at pH 9 and pH 4.

The leaching of BCG from the nanofibres is an important property, especially if the materials are in contact with the wound. The release of BCG from the material to the wound is not a desirable property. For this reason, check the leaching of BCG from the nanofibres by immersing the nanofibres in buffer solutions for 24 h. Briefly, cut the pieces of electrospun nanofibres with the size 1.5 cm^2 and put them in a 2 mL microcentrifuge tube. Then, fill the microcentrifuge tube with 1 mL of buffer, and shake it gently for 24 h (100 rpm). After 24 h, measure the absorbance spectrum in the range from 200 to 800 nm using an UV-Vis spectrophotometer to define the wavelength of maximum absorbance. Test the leaching with the buffers with pH 4, 7 and 9. Perform the experiment in two parallels. For the determination of concentrations of BCG in the buffer solutions, prepare calibration curves of BCG in each buffer at the previoulys determined wavelength of maximum absorbance for each buffer separately.

3.4 Results and discussion

1) **Characterisation of polymer solutions**: Give the measured values of the viscosity, conductivity and surface tension of the CA solution and dye containing CA solution in the form of a Table. Does the addition of BCG into the CA solution influence the solution's viscosity, conductivity or surface tension?
2) **Electrospinning process:** What was the optimal spinning procedure (voltage, electrode distance, electrode rotation speed, ambient humidity, ambient temperature, electrospinning time)?
3) **Characterisation of electrospun mats:**
   i) Prepare a Figure with digital images of electrospun mats before and after immersion in solutions with different pH (pH 2, 4, 7, 9 and 10). What was the colour of the electrospun mat just after the electrospinning process, before the immersion in solutions with different pH? Explain the reason for this colour?

What were the colours of the electrospun mat after the immersion in solutions with different pH? Explain the reason for each colour change.

ii) Prepare a CIE a*–b* plane with the colour coordinates (CIE L*a*b*) for the samples immersed at different pH values (2, 4, 7, 9 and 10).

iii) Prepare a graph with absorbance spectra of BCG in buffers with pH 4 and pH 9. At which wavelength is the isosbestic point in their UV-Visible spectrum?

iv) Prepare a figure with digital images of one piece of electrospun mat after at least two cycles of immersion in buffer solutions with pH 9 and 4. Take a photo after each immersion. Describe the colour intensity after each cycle.

v) What is the finding of the leaching test?

4 Lab exercise 3: 3D Printed structures

4.1 Objective

The aim of Lab Exercise 3 is to prepare a cellulose-based multifunctional biocomposite which is flame retardant, hydrophobic and high load-bearing. Nanofibrillated cellulose (for strength), carboxymethyl cellulose (as a plasticiser and adhesion promoter), citric acid/sodium hypophophite as flame retardants, and alkyl ketene dimer as a hydrophobising agent, will be combined to do this. Subsequently, this mixture will be used for 3D printing**.** The obtained structures will be characterised using light microscopy, flammability and wettability tests. 3D printing will be used to prepare custom-shaped objects with flame retardant properties from renewable resources, which could be used as elements in automotive applications, aviation, as sensors for electronics, or in construction.

4.2 Introduction

Flame retardant polymer materials can prevent flammability or combustion. Polymeric materials such as polyurethane (PU), polylactic acid (PLA), cellulose [35], polyethylene terephthalate (PET) fabrics [36], which are porous and have a larger surface area, can burn relatively easily, releasing a large amount of heat, flames and smoke which pose a safety risk and can threaten human lives and property. Thus, improvements are needed in the

flame-retardant properties of such polymers. A common way to achieve this is to add flame retardants during or after polymer processing. A few examples of early state halogen-based flame retardants are tris(2-chloroethyl) phosphate, tris(1,3-dichloroisopropyl) phosphate, pentabromobenzyl acrylate and tris(1-chloro-2-propyl) phosphate [37]. Even though these materials have been used largely in the commercial products furniture, mattresses, textiles, electronics etc., their production harms the environment, and they produce toxic reaction products such as dioxins and furans upon combustion and disposal. This hampers their usage in the engineering of advanced and safe materials, and alternative flame retardants are required [38]. Several halogen free materials have been used, involving phosphorus, nitrogen, silicone, boron, zinc, iron, and aluminium-containing components. Polymers that contain nitrogen-based flame retardants, for example, can absorb heat, and produce non-combustible gases to dilute the concentration of combustibles during the decomposition process. In addition, they release lower amounts of smoke particles and toxic gases during the combustion [39]. Silicone based flame retardants are also often used in construction applications, since they can easily form an insulating layer on the polymer surface during the burning process, and, thus, limit the transmission of oxygen and heat efficiently, and, therefore, reduce the flammability of polymers [40]. Other flame retardants based on boron [41], zinc [42], aluminium [43] were used for the suppression of smoke particles, and to inhibit the flammability of the polymers. Nonetheless, there are still some bottlenecks in using the above-mentioned flame-retardant materials. For example, increased viscosity and modulus of the final polymeric formulation makes industrial processing difficult. Excess loading of the flame retardant poses a risk to human health and the environment [43]. Therefore, lately, citric-acid/phosphorus-based polymeric materials have been investigated as flame retardant materials in building and construction. When exposed to heat they undergo dehydration and carbonisation to form protective carbon layers, leading to reduced flammability of the polymers [44].

Despite the existence or the commercial availability of synthetic flame-retardant materials, biobased polymeric composites or approaches are needed to release less toxic chemicals upon the burning process. One way to reach this goal is to merge a biobased polymer like cellulose and its derivative with citric acid/phosphonate mixtures.

3D bioprinting is one of the most promising technologies in the area of Additive Manufacturing, which can be used to create 3D materials using polymers and their solutions. 3D printing can be categorised into three major groups, according to their working principles: Extrusion-, droplet-, and laser-based bioprinting (Figure 4.2). Extrusion-based bioprinting utilises mechanical or pneumatic potential energy to extrude a bioink (usually a polymer solution) to overcome surface tension-driven droplet formation, and draw the ink in the form of cylindrical filaments. It can be categorised into (1) **Pneumatic,** (2) Mechanical, or (3) Solenoid microextrusion. Each bioprinting technique has unique features, and possesses certain advantages and disadvantages with respect to printing capabilities, resolution, deposition speed, scalability, bioink and material compatibility, ease of use, printing speed and price, and commercial availability, as well as fundamental aspects of biocompatibility. Compared to other bioprinting techniques, **pneumatic-based extrusion is relatively simple and user-friendly**. It is a combination of fluid dispensing and an automated robotic system for extrusion. A bioink is dispensed by a precise deposition system that allows the formation of 3D custom-shaped structures. The method is suitable for a broad range of materials and for the generation of large, freestanding multifunctional 3D objects or planar microstructures. The properties of the printed structures are defined by manipulation of material viscosity, the nozzle diameter and the applied extrusion pressure [45]. Using the **pneumatic-based extrusion technique, a spatially organised multicomponent structure possessing all the special properties (e.g., mesoporosity, air-trapping voids, vertically aligned pores) can be manufactured, that would allow control of flammability and mechanical durability.**

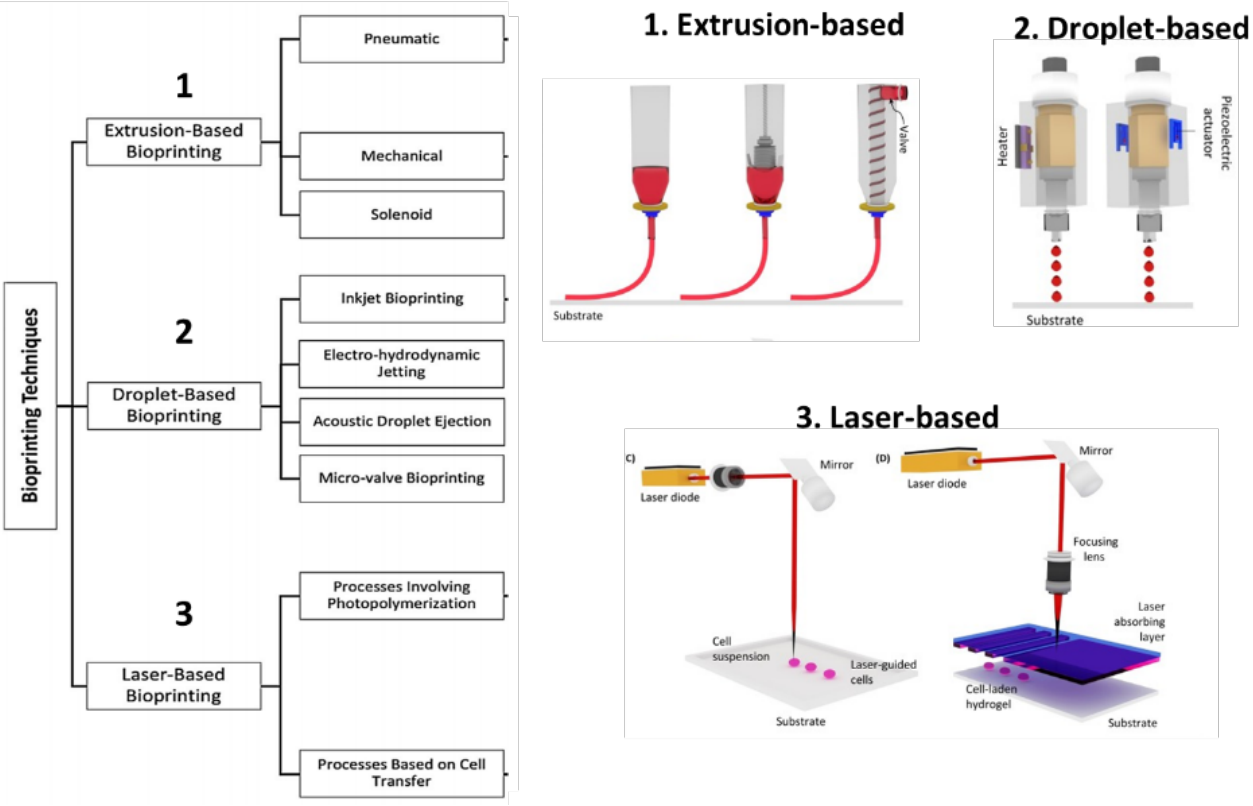

Figure 4.2: Classification of 3D bioprinting

Carboxymethyl cellulose and nanofibrillated cellulose, will be combined to prepare cellulose-based flame retardant biocomposite materials with different shapes. To increase the flame retardant properties of these materials, citric acid and sodium hypophosphite will be mixed in the polymers` solution. Hydrophobic modification is achieved by adding alkyl ketene dimer (AKD). The chemical structures of citric acid, sodium hypophosphite and AKD are shown in Figure 4.3. The 3D bioprinter (BioScaffolder, GESim, Germany) presented in Figure 4.4 is used for the 3D printing of the prepared polymer dispersion.

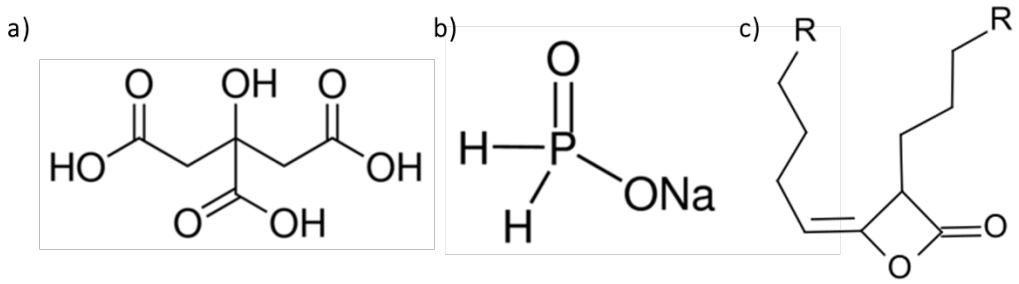

Figure 4.3: Chemical structures of a) citric acid, b) sodium hypophosphite, c) alkyl ketene dimer (AKD).

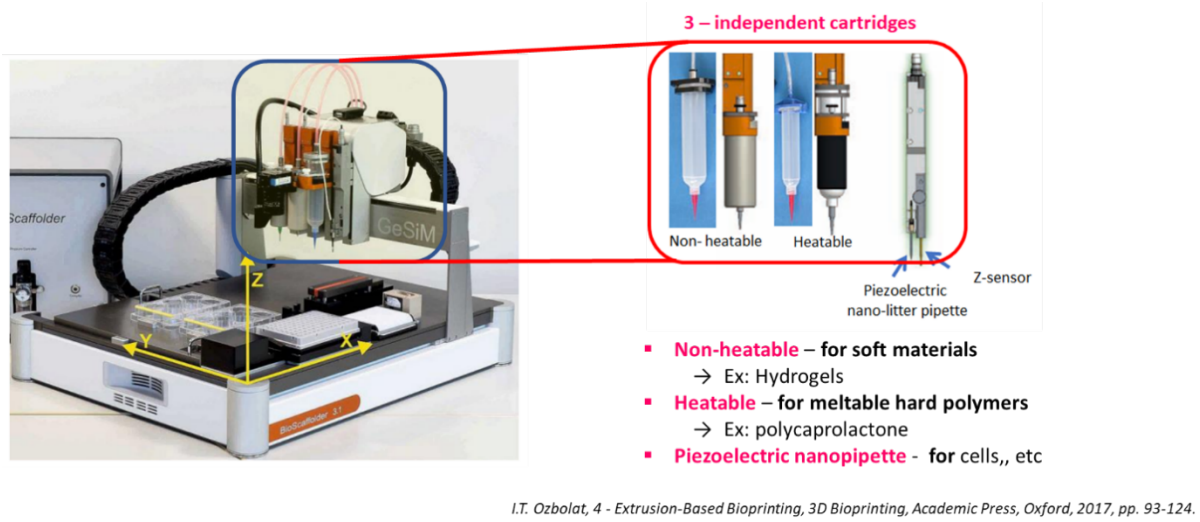

Figure 4.4: A pneumatic micro-extrusion 3D printer

4.3 Experimental section

Materials required

The chemicals and materials needed for the preparation and characterisation of cellulose-based flame retardant biocomposite materials with different shapes are listed below:

- carboxymethyl cellulose (CMC) M_W: 700, 000, D.S: 0.9, Sigma-Aldrich,
- nanofibrillated cellulose (NFC) 3% (w/v), University of Maine, USA,
- citric acid (CitricA), Sigma-Aldrich,
- sodium hypophosphite (SHP), Sigma-Aldrich,
- alkyl ketene dimer (AKD), kemira-KTM d.o.o, Slovenia,
- Milli-Q water from a Millipore water purification system (Millipore, U.S.A; resistivity = 18.2 MΩ·cm),
- mechanical stirrer.

Preparation of 3D printed structures

Preparation of polymer dispersion: Briefly, add (slowly) 10 g of CitricA to 40 g of Milli-Q water, stir until it dissolves. Then, add 10 g of SHP slowly to the CitricA solution and stir until it dissolves. To 44 g of CitricA:SHP solution, add 6 g of CMC (MW: 700, 000 Da, DS 0.9) and stir with a mechanical stirrer (1000-3000 rpm) for 15 min. To this mixture, add 50 g of NFC (3%), stir with a mechanical stirrer (1000-3000 rpm) until no fibres are

visible (ca. 10 min). To this, finally, add 10 g of AKD, stir with a mechanical stirrer (5 min) until a homogeneous paste is obtained.

3D printing: Print the hydrogel/bioink using the 3D bioprinter (BioScaffolder, GESim, Germany). The head consists of a micro valve for accurate dispensing, with a 300 μm diameter nozzle. Control the flow rate by adjusting the dispensing pressure (100−160 kPa), the valve opening time (400−1200 μs), and the dosing distance (0.05−0.07 mm). Control the width of the printed lines by adjusting the parameters mentioned above and the printing speed (10−20 mm/s). Prior to filling the cartridge for each printing, stir the bioink with a spatula to reduce settling. Print different shapes onto polystyrene petri dishes: A small grid (7.2 × 7.2 mm^2, line spacing 1.2 mm, 6 layers), a large grid (38.5 × 17.7 mm^2, 6 horizontal lines with 2.5 mm spacing, 10 vertical lines with 3.5 mm spacing, 1 layer), a solid disc (8 mm diameter, 1.5 mm high, line space 0.5 mm, 5 layers). Measure the dimensions of the 3D printed structures after printing. Design the grids and solid disc in the software (BioScaffolder, GESim) to generate the process protocol for the 3D bioprinter. The grids should use a dosing distance of 0.07 mm, valve opening time of 1200 μs, and printing speed of 20 mm/s. Measure the line width for each grid at 10 different points using a light microscope and the software ImageJ. Freeze the printed samples at -35 °C for 48 h and lyophilise them for 2 d at 10^{-3} mbar and -25 °C. Additionally, put some of the samples in the oven at 120 °C for 24 h, to crosslink the chemical compounds with –OH groups. The crosslinking of AKD will provide hydrophobicity to 3D printed material.

Casting and lyophilisation: As a reference sample (material from pure cellulose), prepare 100 mL of 1.5 % NFC solution. Then cast it in the mould. Freeze the sample at -35 °C for 48 h and lyophilise it for 2 d at 10^{-3} mbar and -25 °C.

Analytical methods

Microscopy analysis of 3D printed materials: Analyse the microporous structures of the prints by microscopy using an Olympus BX51 microscope (Olympus U-MWIB filter cube). The analysis should be performed with the help of a qualified person.

Wettability: Define the hydrophilic/hydrophobic properties of the pure cellulose material (casted and lyophilised) and 3D printed material with deposition of a water drop on the surface of the material.

Flammability test: Flammability testing is the principle way to determine how easily a material will ignite or burn when placed or used in close proximity to fire or heat. Flammability testing actually covers a number of different testing methods (ASTM D2863, ISO 3795) intended to measure a material's specific vulnerability, including its susceptibility to an ignition source, its propensity to combust, and the rate at which it will burn when ignited.

In this Lab Exercise, measure the rate of burning for a pure cellulose sample and 3D printed sample. Briefly, take an equal mass of pure cellulose and 3D printed material and expose them to the fire source. Measure the time needed for the decomposition of all material. Also, pay attention to whether the sample is burning or extinguishing after fire source removal.

4.4 Results and discussion

Microscopy analysis: Give the results obtained from the optical microscopy measurements – give the microscopy images for scaffold samples NFC-CMC-CitricA-SHP-AKD printed at different pressures. Calculate the pore sizes from the images and give them as a Table or graph. Does pressure effect the pore size? How?

Wettability: Take a photo of the surface of the pure cellulose material (casted and lyophilised NFC) and 3D printed sample immediately after deposition of a water drop on the surface of the material. Describe the hydrophilic/hydrophobic character of both materials.

Flammability test: Take a photo of the pure cellulose material (casted and lyophilised NFC) and 3D printed sample during the flammability test. Describe the process of burning for both materials.

References

1. Blanco, I., *Lifetime Prediction of Polymers: To Bet, or Not to Bet—Is This the Question?* Materials, 2018. 11(8): p. 1383.
2. Al-Zahrani, M.M., et al., *Mechanical properties and durability characteristics of polymer- and cement-based repair materials.* Cement and Concrete Composites, 2003. 25(4): p. 527-537.
3. Gourlay, S.J., et al., *Biocompatibility testing of polymers: In vivo implantation studies.* Journal of Biomedical Materials Research, 1978. 12(2): p. 219-232.
4. McAndrew, T.P., *Corrosion prevention with electrically conductive polymers.* Trends in Polymer Science, 1997. 1(5): p. 7-12.
5. Pearce, E., *Flame-retardant polymeric materials.* 2012: Springer Science & Business Media.
6. Belgacem, M.N. and A. Gandini, *Monomers, polymers and composites from renewable resources.* 2011: Elsevier.
7. Liang, S., et al., *Flame retardancy and thermal decomposition of flexible polyurethane foams: Structural influence of organophosphorus compounds.* Polymer Degradation and Stability, 2012. 97(11): p. 2428-2440.
8. Wang, H., G. Gurau, and R.D. Rogers, *Ionic liquid processing of cellulose.* Chemical Society Reviews, 2012. 41(4): p. 1519-1537.
9. Klemm, D., et al., *Cellulose: Fascinating Biopolymer and Sustainable Raw Material.* Angewandte Chemie International Edition, 2005. 44(22): p. 3358-3393.
10. Sehaqui, H., L.A. Berglund, and Q. Zhou, *Biorefinery: Nanofibrillated cellulose for enhancement of strength in high-density paper structures.* Nordic Pulp & Paper Research Journal, 2013. 28(2): p. 182-189.
11. Mohan, T., *Nanometric Cellulosic Layers for Specific Adsorption of Polysaccharides and Immobilization of Bioactive Molecules: Doctoral Dissertation.* 2012, T. Mohan.
12. Cooper, G.K., K.R. Sandberg, and J.F. Hinck, *Trimethylsilyl cellulose as precursor to regenerated cellulose fiber.* Journal of Applied Polymer Science, 1981. 26(11): p. 3827-3836.
13. Mohan, T., et al., *Wettability and surface composition of partly and fully regenerated cellulose thin films from trimethylsilyl cellulose.* Journal of Colloid and Interface Science, 2011. 358(2): p. 604-610.
14. Kontturi, E., P.C. Thüne, and J.W. Niemantsverdriet, *Novel method for preparing cellulose model surfaces by spin coating.* Polymer, 2003. 44(13): p. 3621-3625.
15. Benchabane, A. and K. Bekkour, *Rheological properties of carboxymethyl cellulose (CMC) solutions.* Colloid and Polymer Science, 2008. 286(10): p. 1173.
16. Habib, A., et al., *3D Printability of Alginate-Carboxymethyl Cellulose Hydrogel.* Materials (Basel), 2018. 11(3).
17. Maver, T., et al., *Electrospun nanofibrous CMC/PEO as a part of an effective pain-relieving wound dressing.* Journal of Sol-Gel Science and Technology, 2016. 79(3): p. 475-486.
18. Gašparič, P., et al., *Nanofibrous polysaccharide hydroxyapatite composites with biocompatibility against human osteoblasts.* Carbohydrate Polymers, 2017. 177: p. 388-396.

19. Sharma, A., et al., *Commercial application of cellulose nano-composites – A review*. Biotechnology Reports, 2019. 21: p. e00316.
20. Fischer, S., et al. *Properties and applications of cellulose acetate*. in *Macromolecular Symposia*. 2008. Wiley Online Library.
21. Taepaiboon, P., U. Rungsardthong, and P. Supaphol, *Vitamin-loaded electrospun cellulose acetate nanofiber mats as transdermal and dermal therapeutic agents of vitamin A acid and vitamin E*. European Journal of Pharmaceutics and Biopharmaceutics, 2007. 67(2): p. 387-397.
22. Lee, H., S.B.A. Hamid, and S. Zain, *Conversion of lignocellulosic biomass to nanocellulose: structure and chemical process*. The Scientific World Journal, 2014. 2014.
23. Abdul Khalil, H.P.S., et al., *Production and modification of nanofibrillated cellulose using various mechanical processes: A review*. Carbohydrate Polymers, 2014. 99: p. 649-665.
24. Phanthong, P., et al., *Nanocellulose: Extraction and application*. Carbon Resources Conversion, 2018. 1(1): p. 32-43.
25. *Dataphysics*. 2018; Available from: https://www.dataphysics-instruments.com/products/oca/.
26. Maver, T., et al., *Emerging Techniques in the Preparation of Wound Care Products*, in *Bioactive Polysaccharide Materials for Modern Wound Healing*, T. Maver, et al., Editors. 2018, Springer International Publishing: Cham. p. 25-38.
27. Bennison, L., et al., *The pH of wounds during healing and infection: a descriptive literature review*. Wound Practice & Research: Journal of the Australian Wound Management Association, 2017. 25(2): p. 63.
28. Duncan, T.V., *Applications of nanotechnology in food packaging and food safety: barrier materials, antimicrobials and sensors*. Journal of colloid and interface science, 2011. 363(1): p. 1-24.
29. Van der Schueren, L., et al., *Polycaprolactone and polycaprolactone/chitosan nanofibres functionalised with the pH-sensitive dye Nitrazine Yellow*. Carbohydrate Polymers, 2013. 91(1): p. 284-293.
30. Dargaville, T.R., et al., *Sensors and imaging for wound healing: A review*. Biosensors and Bioelectronics, 2013. 41(Supplement C): p. 30-42.
31. Kurečič, M. and M.S. Smole, *Electrospinning: Nanofibre Production Method*. Tekstilec, 2013. 56(1).
32. N., S., et al., *Flame-retardant fabric systems based on electrospun polyamide/boric acid nanocomposite fibers*. Journal of Applied Polymer Science, 2012. 126(2): p. 614-619.
33. *Fiber Generators in Needleless Electrospinning*. Journal of Nanomaterials, 2012. 2012: p. 13.
34. Schanda, J., *Colorimetry: understanding the CIE system*. 2007: John Wiley & Sons.
35. Alongi, J., et al., *Intrinsic intumescent-like flame retardant properties of DNA-treated cotton fabrics*. Carbohydrate Polymers, 2013. 96(1): p. 296-304.
36. Chen, D.-Q., et al., *Flame-retardant and anti-dripping effects of a novel char-forming flame retardant for the treatment of poly(ethylene terephthalate) fabrics*. Polymer Degradation and Stability, 2005. 88(2): p. 349-356.
37. Dvir, H., et al., *Optimization of a flame-retarded polypropylene composite*. Composites Science and Technology, 2003. 63(13): p. 1865-1875.
38. Hooshangi, Z., S.A.H. Feghhi, and N. Sheikh, *The effect of electron-beam irradiation and halogen-free flame retardants on properties of poly butylene terephthalate*. Radiation Physics and Chemistry, 2015. 108: p. 54-59.
39. Horacek, H. and R. Grabner, *Advantages of flame retardants based on nitrogen compounds*. Polymer Degradation and Stability, 1996. 54(2): p. 205-215.
40. Wang, S., et al., *Preparation and characterization of flame retardant ABS/montmorillonite nanocomposite*. Applied Clay Science, 2004. 25(1): p. 49-55.
41. Gao, X., et al., *Synthesis and characterization of polyurethane/zinc borate nanocomposites*. Colloids and Surfaces A: Physicochemical and Engineering Aspects, 2011. 384(1): p. 2-8.
42. Qiu, X., et al., *Flame retardant coatings prepared using layer by layer assembly: A review*. Chemical Engineering Journal, 2018. 334: p. 108-122.
43. Shi, Z., et al., *Thermal conductivity and fire resistance of epoxy molding compounds filled with Si3N4 and Al(OH)3*. Materials & Design, 2012. 34: p. 820-824.
44. Wu, K., et al., *Flame Retardancy and Thermal Degradation of Intumescent Flame Retardant Starch-Based Biodegradable Composites*. Industrial & Engineering Chemistry Research, 2009. 48(6): p. 3150-3157.
45. Mohan, T., et al., *6 - 3D bioprinting of polysaccharides and their derivatives: From characterization to application*, in *Fundamental Biomaterials: Polymers*. 2018, Woodhead Publishing. p. 105-141.

Design, Characterisation and Applications of Cellulose-Based Thin Films, Nanofibers and 3D Printed Structuresv: A Laboratory Manual

Tanja Pivec[1], Tamilselvan Mohan[1], Rupert Kargl[1], Manja Kurečič[2] & Karin Stana Kleinschek[2]

[1] University of Maribor, Faculty of Mechanical Engineering, Maribor, Slovenia.
E-mail: tanja.pivec@um.si, tamilselvan.mohan@um.si, rupert.karl@um.si, karin.stana@um.si
[2] University of Maribor, Faculty of Electrical Engineering and Computer Science, Maribor, Slovenia. E-mail: manja.kurecic@um.si, karin.stanakleinschek@tugraz.at

Abstract The introduction of the Laboratory Manual gives the theoretical bases on cellulose and its derivatives, which are used as starting polymers for the preparation of multifunctional polymers with three different advanced techniques - spin coating, electrospinning and 3D printing. In the following, each technique is presented in a separate Lab Exercise. Each exercise covers the theoretical basics on techniques for polymer processing and methods for their characterisation, with an emphasis on the application of prepared materials. The experimental sections contain all the necessary information needed to implement the exercises, while the added results provide students with the help to implement correct and successful exercises and interpret the results.

Keywords: polysaccharides, cellulose, electrospun, spin-coating, 3D printing, nanofiber, thin films, multifunctional materials.

University of Maribor Press

DOI https://doi.org/10.18690/978-961-286-432-3 ISBN 978-961-286-432-3

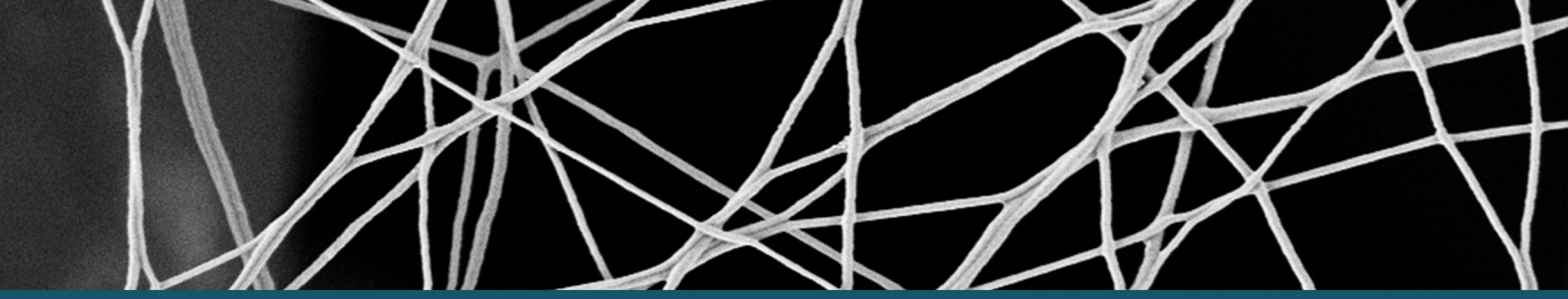

University of Maribor

Faculty of Mechanical Engineering

A comparison of SWCA for TMSC and cellulose films is presented in Figure 1.1. SWCA of a typical TMSC film is 98.0 ± 2.8 °, of a cellulose film 25.0 ± 0.6 °, meaning that the hydrophilicity was increased after acidic hydrolysis of the silylether groups, indicating that the cellulose film was regenerated.

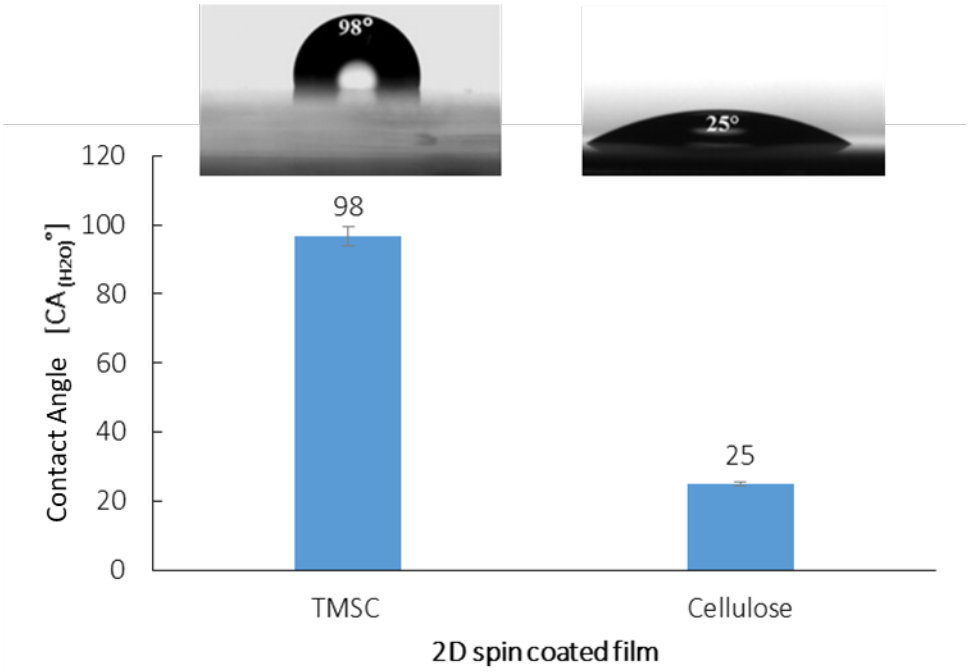

Static Water Contact Angles (SWCA) on TMSC and regenerated cellulose films.

Characterisation of polymer solutions: The addition of BCG into the CA electrospinning solution (17 wt% CA; 85% AcOH) should not influence the solution's viscosity, conductivity and surface tension, and it should not hinder the electrospinning process.

Electrospinning process: The optimal spinning procedure should be as follows: Voltage: 75 kV, Electrode distance: 160 mm, electrode rotation speed: 3.8 rpm, ambient humidity: 30%, ambient temperature: 20°C and electrospinning time: 40 min.

Characterisation of electrospun mats: Figure 1.2 a) shows the electrospun mats before and after immersion in solutions with different pH. From Figure 3.3 a) it can be observed that the CA nanofibrous mats with incorporated BCG (Figure 1.2 a)– before) is slightly yellow just after the electrospinning process, caused by the acidic conditions during fibre formation (acetic acid). The colour of the electrospun mat with included BCG and dipped in both acidic solutions (pH 2 and 4), where BCG occurs in its protonated form (see Figure 3.2), is intense yellow (Figure 1.2 a) – after). The colour of the sample immersed into alkaline solutions (pH 9 and 10, non-protonated BCG) is blue. The green colour of the sample at pH 7 is due to the fact that both species (protonated and non-protonanted BCG) are present in such quantities that the observed colour originates from a combination of yellow and blue.

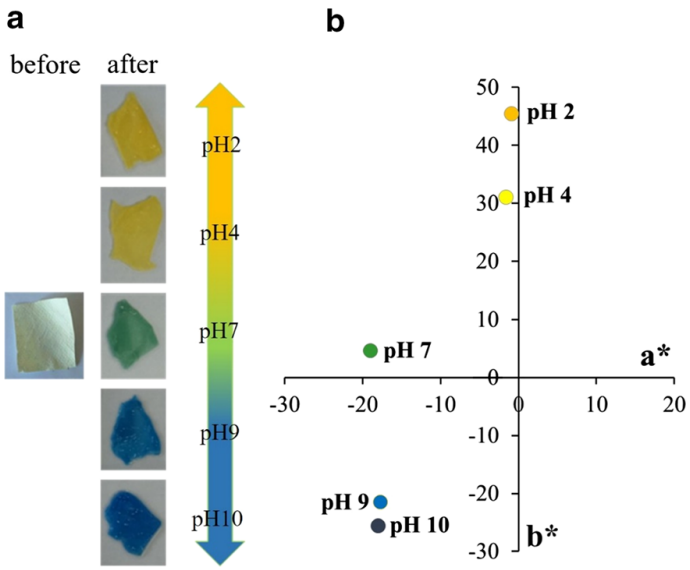

The coloured nanofibres depending on the solutions' pH: a) Samples' photographs before and after immersion in pH solutions; b) Position of samples in the CIE a*–b* plane.

The results from the colour measurements and colour coordinates (CIE L*a*b*) for the samples immersed at different pH values (2, 4, 7, 9 and 10) are depicted in Fig. 1.2 b). From Figure 1.2 b) it can be seen that, after the immersion of the electrospun mat in acidic pH, the lower the pH of solution is, the more intensive is the yellow colour of electrospun mat, while, at the same time, the blue colour lost its intensity (higher b* value); and vice versa, after immersion of electrospun mat in alkaline pH, the higher the pH of solution is, the lower is the obtained b*value. The neutral solution (pH 7) led to a green hue of the sample, i.e. a* is - 18.94 and b* is 4.51, although the dye producer declares that the BCG solution has a visual transition interval (green colour) at lower pH values (3.8–5.4). It should be kept in mind that the halochromic behaviour of the BCG in the surrounding CA matrix altered compared to its behaviour in solution, which is most likely attributed to the dye-polymer interactions [46], as well as the different accessibility of the dye molecules in the nanofibrous materials (compared to its molecular dispersion).

Figure 1.3 a) shows the absorbance spectra of BCG in buffers with pH 4 (yellow) and pH 9 (blue). The acid and basic forms of BCG have an isosbestic point in their UV-Visible spectrum, around 540 nm, indicating that the two forms interconvert directly without forming any other substance. Figure 1.3 b) shows the electrospun mat after two cycles of immersion in buffer solutions with pH 9 and 4. The colour of the electrospun mat after dipping in buffer solution with pH 9 is blue. Then, the sample was transferred to buffer solution with pH 4, and the colour was changed to yellow. Then, the sample was transferred again in buffer solution with pH 9, and the colour changed to blue with the same intensity as in the first cycle. After immersion in buffer solution with pH 4 in the second cycle, the colour changed again to yellow with the same intensity as in the first cycle.

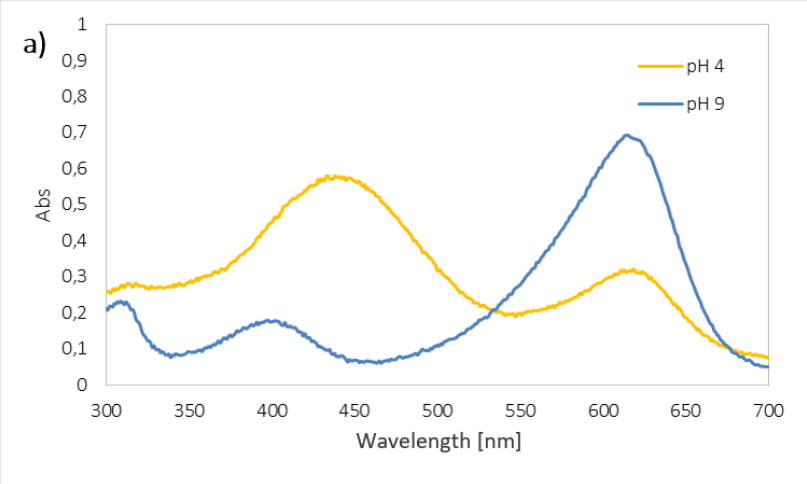

a) UV-Vis spectra of BCG in buffers with pH 4 (yellow) and pH 9 (blue), b) The electrospun mat after two cycles of immersion in buffer solutions with pH 9 and 4.

The leaching test showed that the concentration of BCG in buffers was below the detection limit, since no peak was detected in the wavelength from 200 to 800 nm.

Microscopy analysis: Figure 1.4 shows the results obtained from the optical microscopy measurements of 3D printed scaffolds using NFC-CMC-CitricA-SHP-AKD at different printing pressures. The microscopy images for samples printed at different pressures are shown in the left side. The pore sizes calculated from the images are given on the right side. Results show that the pore size of the printed structures can be tuned by simply tuning the pressure. A higher pore size is observed at lower pressure (160 kPa). At 200 kPa, no pores are detected due to closing of the print.

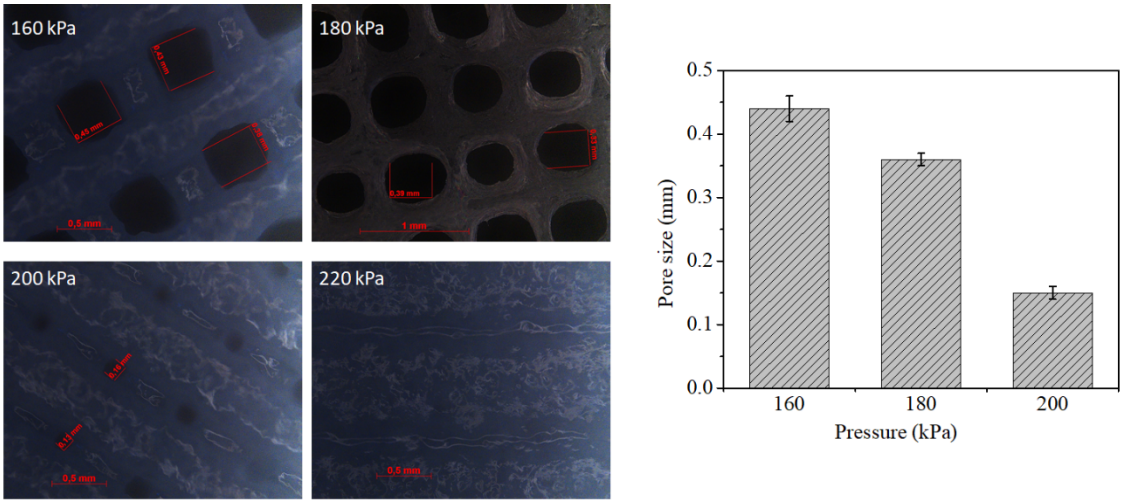

Left side – microscopy images and pore size of the 3D printed structures.

Wettability: Figure 1.5 (a) shows the surface of pure cellulose material (casted and lyophilised NFC) immediately after deposition of a water drop on the surface of the material. One can observe that the water drop is absorbed into the material immediately, meaning that the material is hydrophilic. Figure 1.5 (b) shows the surface of a 3D printed sample (NFC-CMC-CitricA-SHP-AKD after heat curing) after the placement of three water drops on the surface of the material. The drops are not absorbed into the material, meaning that the material is hydrophobic.

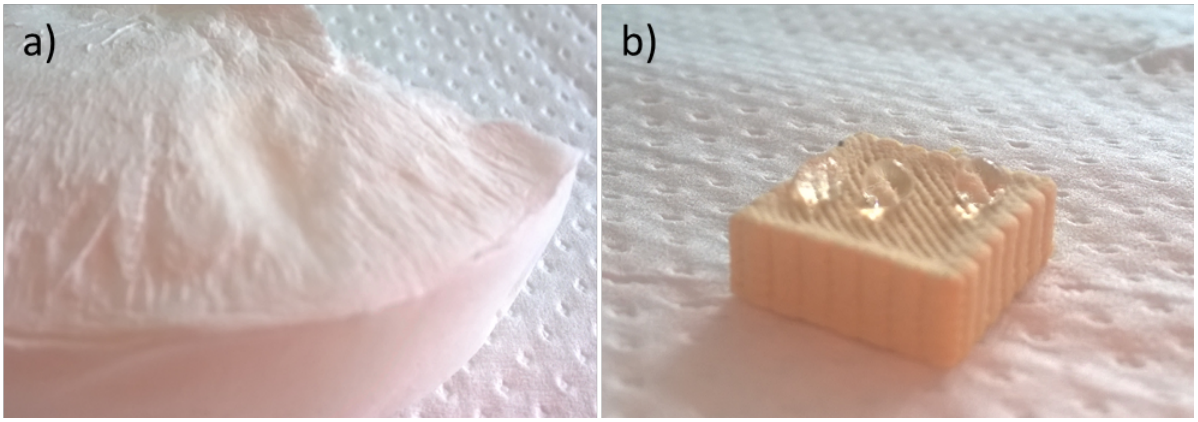

Hydrophilic pure cellulose material (a); hydrophobic 3D printed flame retardant material (b).

Flammability test: Figure 1.6 (a) shows the pure cellulose material (casted and lyophilised NFC) which burns fast by spreading the flame over the whole material after removal of the ignition source. Figures 1.6 (b and c) show the flame retardant 3D printed material, where the fire is extinguished after the ignition source is removed.

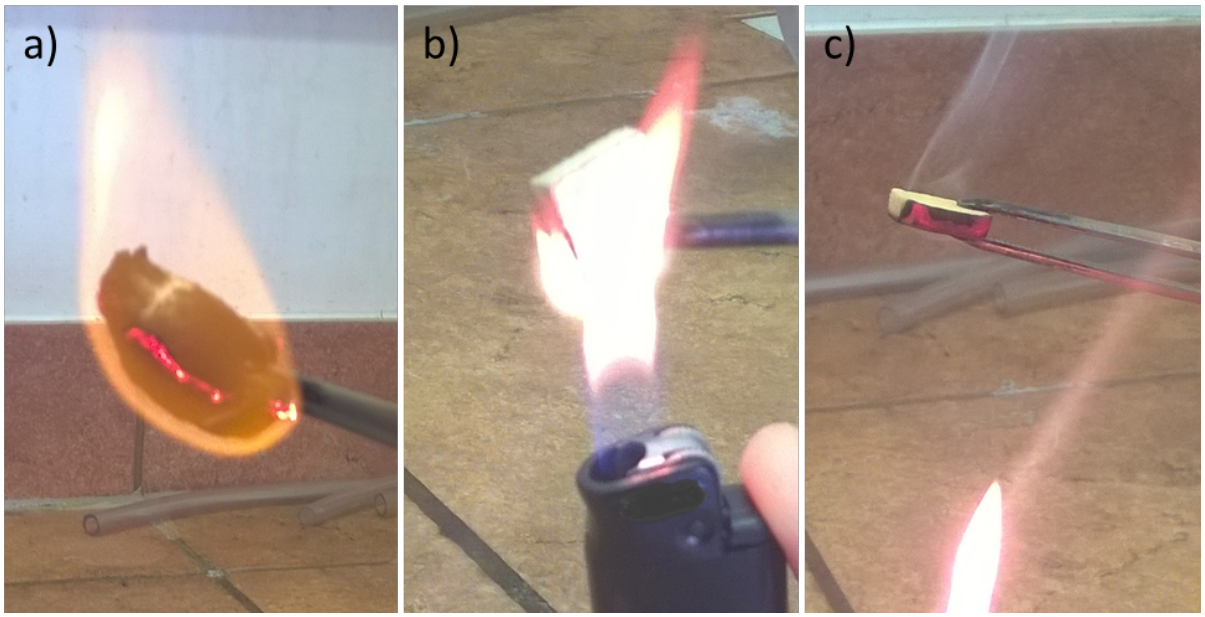

Flammable pure cellulose material (a); flame retardant 3D printed material (b and c).